Int. J. Electrochem. Sci., 15 **(2020)** 2449 – 2457, doi: 10.20964/2020.03.57

International Journal of
ELECTROCHEMICAL
SCIENCE
www.electrochemsci.org

Short Communication

Enhanced Glucose Electrooxidation at Ni-Cu Binary Oxide Nanocatalyst

Mahmoud M. Abuzaied[1], *Yasser M. Asal*[1], *Ahmad M. Mohammad*[2], *Islam M. Al-Akraa*[1,*]

[1] Department of Chemical Engineering, Faculty of Engineering, The British University in Egypt, Cairo 11837, Egypt
[2] Chemistry Department, Faculty of Science, Cairo University, Cairo 12613, Egypt
[*]E-mails: islam.ahmed@bue.edu.eg (Islam M. Al-Akraa); ammohammad@cu.edu.eg (Ahmad M. Mohammad)

Received: 17 November 2019 / *Accepted:* 21 December 2019 / *Published:* 10 February 2020

The aim of this study is to fabricate a nickel (NiOx) and copper (CuOx) oxide nanocatalyst on a glassy carbon (GC) electrode (will be abbreviated as Ni-Cu/GC) for glucose oxidation (GO). A sequential electrodepositon mode was applied to assemble NiOx and CuOx in the fabrication scheme. The optimization of Ni loading on the GC surface (will be abbreviated as Ni/GC electrode) was achieved first to attain the maximum catalytic efficiency in terms of the specific current toward GO. This (409 Ag^{-1})was obtained by applying 15 mC/cm^2 in the deposition of Ni. However, unfortunately the NiOx/GC could not support a long-term stability toward GO that motivated a further modification with CuOx beneath NiOx (will be abbreviated as Ni-Cu/GC electrode). This modification enhanced the stability toward the GO where the decay in the specific current was not too much compared with that of the Ni/GC electrode. After 1 h of continuous electrolysis, the specific current reached 317 Ag^{-1} at the Ni-Cu/GC electrode compared to 167 Ag^{-1} at the Ni/GC electrode.

Keywords: Glucose electro-oxidation; NiOx; CuOx; Catalytic activity; Stability.

1. INTRODUCTION

The ever-increasing demand of energy that resulted with the rapidly growing population and the advanced civilization together with the stringent environmental legislations and regulations to minimize harmful ejections to the environment have motivated research in clean energy production [1, 2]. In fact, fuel cells (FCs) with their simple operation, fast robustness, high efficiency, moving flexibility and convenient reliability have appeared promising for a wide range of portable, stationary and emergency backup power applications [3-7]. They also represented a unique solution for distributing power

generating technologies rather than to transmit electricity over long high voltage lines which costs infrastructure and gets subjected to inherent loses over these long lines.

Fundamentally, FCs operate simply like a galvanic cell in which an electrochemical reaction between a fuel and an oxidant stimulate the production of electricity but reactants are continuously fed in the cell. From the anodic perspective, anything (e.g., gasoline, diesel and biodiesel, propane, hydrogen, formic acid, methanol and glucose) that can be oxidized at an electrode can be used as a fuel [8-17]. Nonetheless, a proper selection for a certain fuel for a specific application should consider the fuel's availability, cost, toxicity, calorific value, storage, density, phase, water content, purity, security of supply, and carbon content. Accordingly, hydrogen (the lightest carbon-free fuel) which has been maintained for long time the ideal fuel in H_2/O_2 FCs may not continue due to challenges in safety associating its use, storage and transportation in addition to its low energy density as a gaseous fuel.

Glucose electro−oxidation (GO) has recently appeared interesting not only for applications in direct glucose FCs (DGFCs) but also for glucose sensing in medical applications [18, 19]. In fact, GO represented a principal reaction in several microbial and enzymatic FCs [20-26]. Nevertheless, their poor performances which originated from the limited life-time of enzymes and sluggish electron transfer from the microbe to the electrode turned out into an unacceptable durability [24, 26-28]. That motivated research for the direct GO on noble metals and metal oxides because of their captivating properties for a lot of applications [29-32]. Candidates in this regard included Au, Ag, Ni, Pd and manganese oxide but Au retained fascinating incomparable activity for GO [27].

Herein, we report on the fabrication of a NiOx and CuOx modified catalyst that owned a fascinating enhanced catalytic activity toward GO. The sequential electrodeposition as a cheap, controllable and facile technique for the assembly of nanostructures was employed in the catalyst's fabrication. With this catalyst, a catalytic efficiency for GO up to 317 Ag^{-1} was achieved.

2. EXPERIMENTAL

Glassy carbon (d = 5.0 mm) electrode served as the working electrodes. An Ag/AgCl/KCl(sat) and a spiral Pt wire were used as reference and counter electrodes, respectively. Conventional procedure was applied to clean the GC electrode as described previously [33] .

At the Ni/GC electrode, the electrode's modification with NiOx was attained in two successive steps. The first one involved assembling of metallic nickel on the GC electrode from an aqueous solution of 0.1 M acetate buffer solution (ABS, pH = 4.0) containing 0.1 M $NiSO_4$ by a constant potential electrolysis at −1 V. several Ni deposition charges (5, 10, 15, 20 and 25 mC/cm^2) were applied during this step. Next, the metallic Ni was oxidized in 0.1 M phosphate buffer solution (PBS, pH = 7) by scanning the potential between −0.5 and 1 V for 10 cycles at 100 mV s^{-1}. While at the Ni-Cu/GC electrode, the electrode's modification with NiOx was attained using the same previous procedures. After that the modification with CuOx was carried out in 0.1M H_2SO_4 solution containing 1.0 mM $CuSO_4$ at a constant potential of − 0.2 V.

The electrochemical measurements were carried out in a traditional three-electrode glass cell at room temperature (around 25 °C) using a BioLogic SAS potentiostat (model SP-150) operated with EC-

lab® software. The catalytic performance of the modified electrodes towards GO was investigated in 0.5 M NaOH solution containing 50 mM glucose.

A scanning electron microscope (SEM, Joel GSM-6610LV, Japan) joined with an energy dispersive X-ray spectrometer (EDS, with accelerating voltage 30 K.V with original magnification ×500, ISIS Company, Oxford, England) was engaged to determine the electrode surface morphology and composition, respectively. The crystal structure of the modified Ni-Cu/GC electrode is identified using XRD (PANalyticalX'Pert PRO instrument, Cu Kα radiation (λ = 1.5404 Å).

3. RESULTS AND DISCUSSION

3.1. Electrochemical characterization

Figure 1 shows CVs obtained at (a) bare GC and (b-f) Ni/GC electrodes. Ni was deposited with different charges (Q) (5-25 mC/cm^2). The measurements are carried out in an alkaline medium to properly monitor the oxidation/reduction behavior of the electrodeposited Ni at the GC surface. A redox couple attributed to the transformation between the lower and the higher oxidation states of Ni is observed (Eqs. 1 and 2) at 0.45 and 0.25 V which confirms the successful deposition of Ni over the GC electrode. A second observation is the current increase along with increasing the Ni deposition charge which tells about increasing the active sites for the redox transformation process [34].

$$Ni(OH)_2 + OH^- \longleftrightarrow NiOOH + H_2O + e^- \quad (1)$$

$$Ni(OH)_2 \longleftrightarrow NiOOH + H^+ + e^- \quad (2)$$

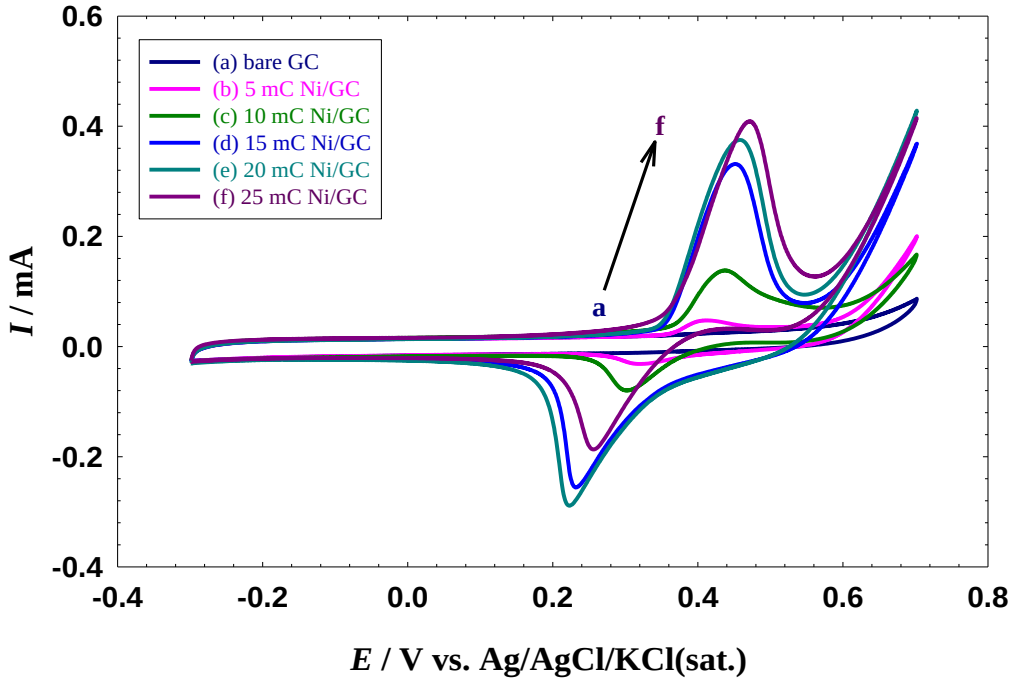

Figure 1. CVs measured in 0.5 M NaOH solution at a scan rate of 50 mVs^{-1} for (a) bare GC electrode and (b-f) Ni/GC electrodes. Ni was deposited with different charges (*Q*) (5-25 mC/cm^2).

3.2. Material characterization

Morphologically, Fig. 2A and B shows FE-SEM images of the Ni/GC and Ni-Cu/GC electrodes at which a 15 mC/cm^2 of Ni has been electrodeposited, respectively. Both figures show a clear view about the deposition of the NiOx at the GC surface in a 90 nm cauliflower-like structure. On the other hand, Fig. 2B shows the deposition of CuOx onto the GC surface in a spongy nanowire-like structure. The EDS analysis in Fig. 3 inferred about the successful deposition of the catalyst ingredients and assisted in calculation of its relative ratios. The peaks of C, O, Ni and Cu appeared on their assigned positions and their relative ratios summarized in the table inserted as inset of Fig. 3.

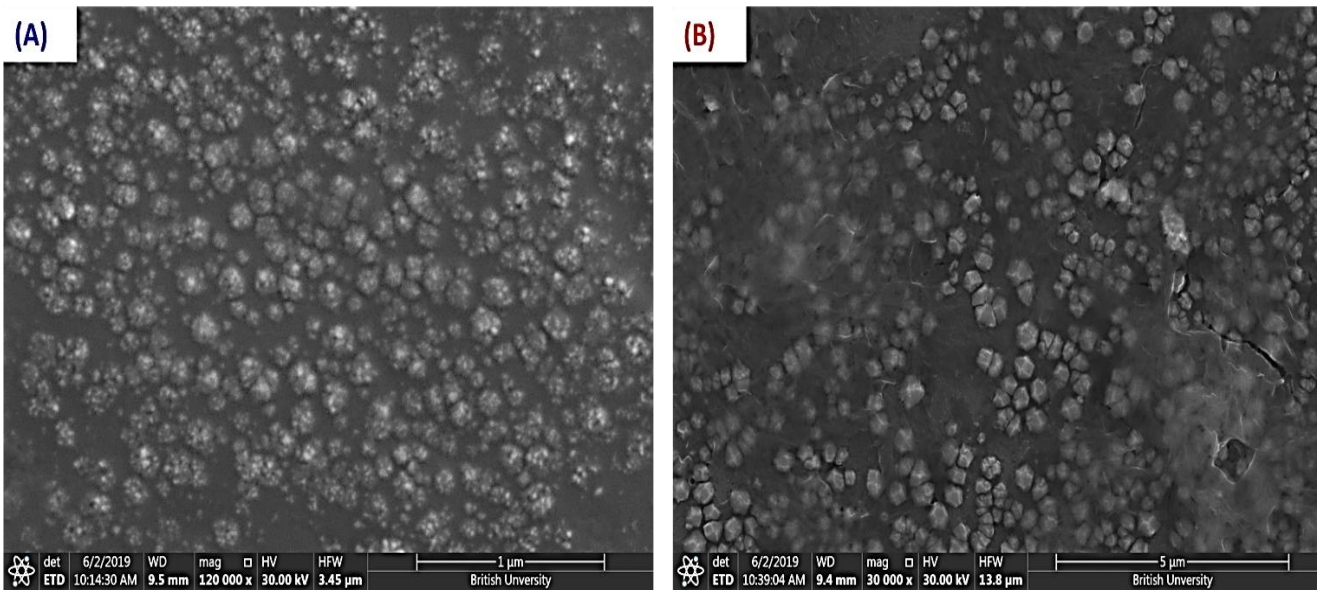

Figure 2. SEM images of the (A) Ni/GC and (B) Ni-Cu/GC electrodes at which a 15 mC/cm^2 of Ni has been electrodeposited.

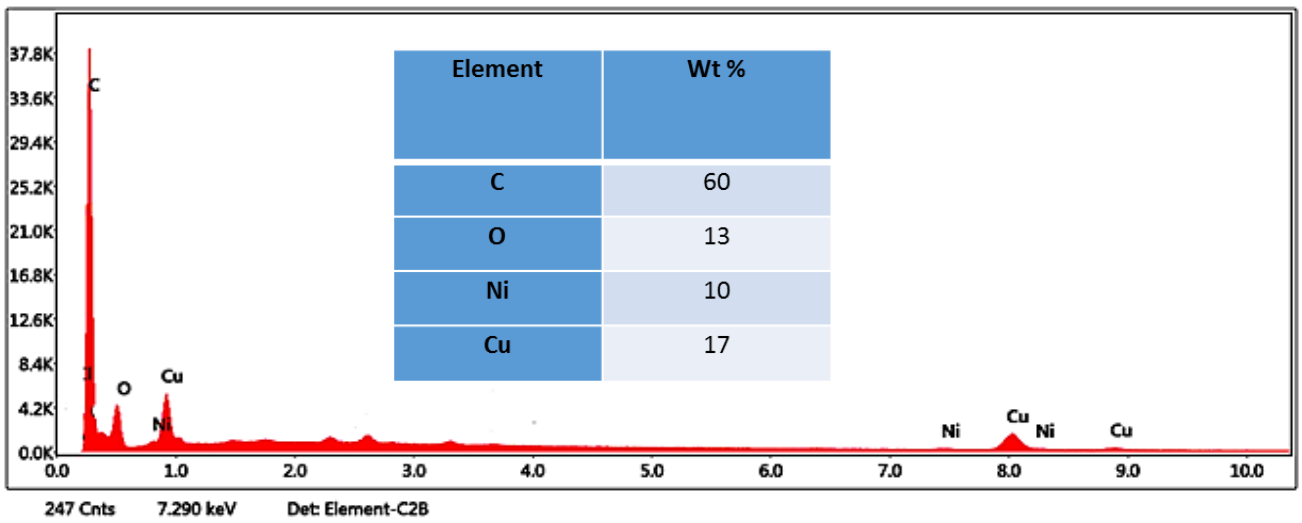

Element	Wt %
C	60
O	13
Ni	10
Cu	17

Figure 3. EDS analysis of the Ni-Cu/GC electrodes at which a 15 mC/cm^2 of Ni has been electrodeposited.

The crystal structure of the Ni-Cu/GC electrode is identified by XRD as shown in Fig. 4. The broad peaks at ca. 2θ 25° and 78 ° are related to the glassy carbon support. The three sharp peaks appeared at ca. 43.3°, 50.6° and 74.2° are related to Ni (111), (002) and (022) planes of Ni where the small sharp peak at ca. 36.5° is related to the cuprite (111) plane [35, 36].

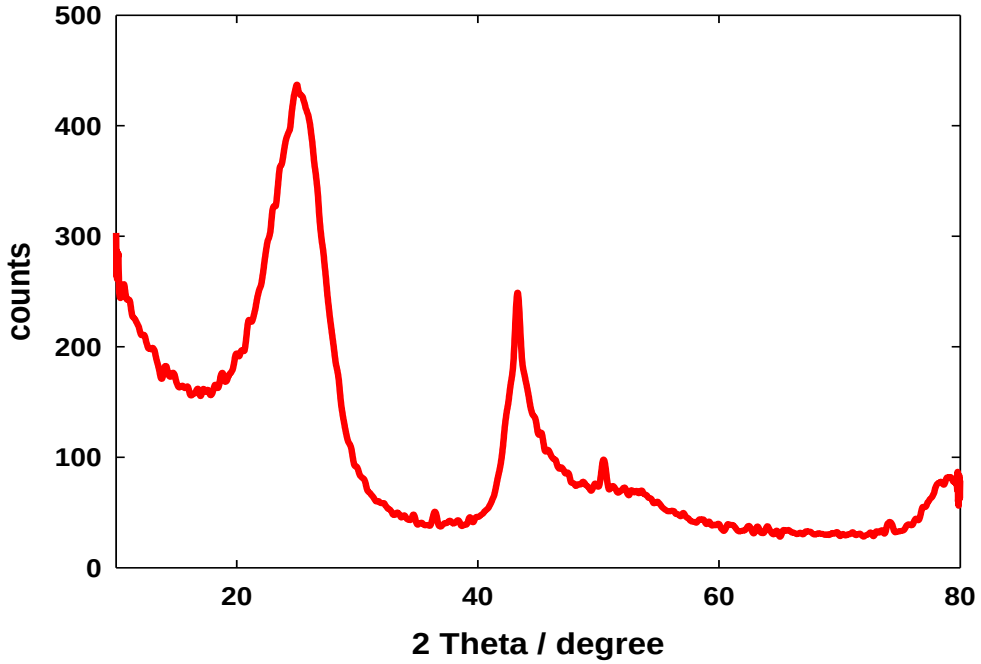

Figure 4. XRD analysis of the Ni-Cu/GC electrodes at which a 15 mC/cm^2 of Ni has been electrodeposited.

3.2. Electrocatalysis of GO

The electrocatalytic activity towards GO has been investigated firstly at the Ni/GC electrode in 0.5 M NaOH containing 50 mM glucose. The optimization of the Ni charge loading towards GO has been plotted in Fig. 5. Fig. 5 a (for bare GC electrode) showed that the GC electrode itself is completely inactive towards GO under the current conditions.

In contrast, at the Ni/GC electrodes (Fig. 5 b-f), the GO is significantly enhanced indicating that the NiOx is essential for providing the suitable adsorption sites for GO. It is believed that are firstly adsorbed at the NiOx active sites then oxidized to gluconolactone at higher potential simultaneously with the transformation of $Ni(OH)_2$ to NiOOH [37]. In other words, NiOx act as a catalytic mediator facilitating the GO process (Eqs. 3 and 4).

$$Ni^{2+} \longrightarrow Ni^{3+} + e^- \quad (3)$$

$$Ni^{3+} + \text{glucose} \longrightarrow \text{gluconolactone} + Ni^{2+} \quad (4)$$

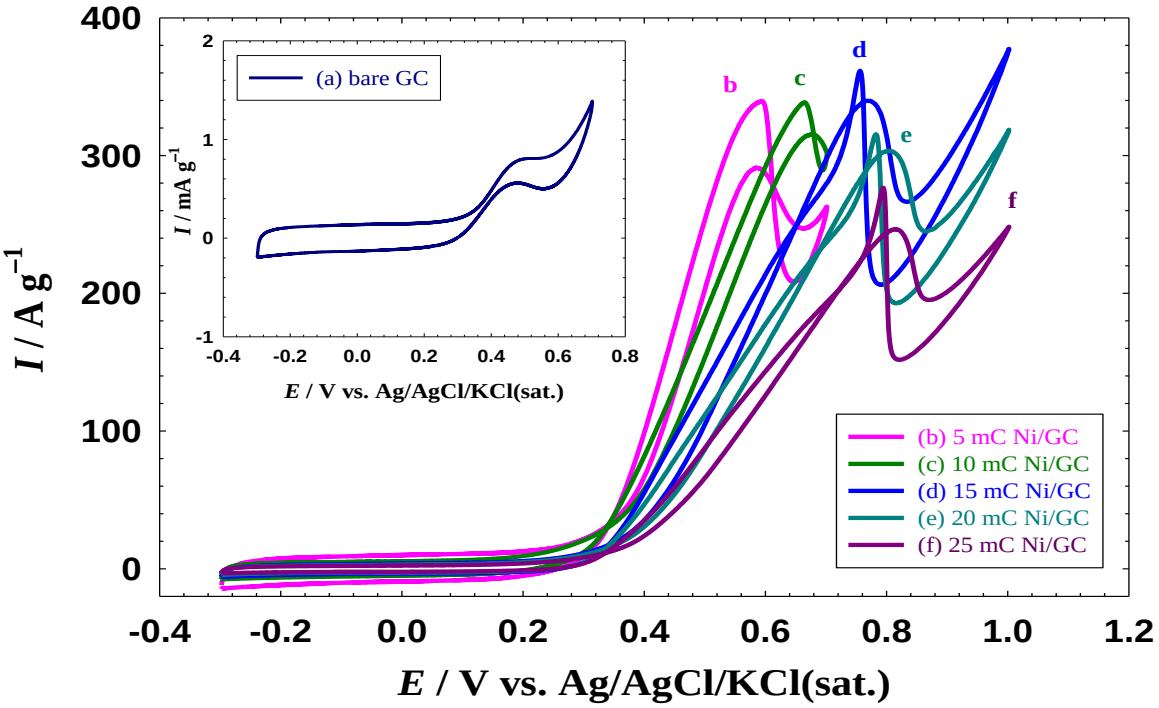

Figure 5. CVs measured in 0.5 M NaOH solution containing 50 mM glucose at a scan rate of 100 mVs^{-1} for (a) bare GC electrode and (b-f) Ni/GC electrodes. Ni was deposited with different charges (Q) (5-25 mC/cm^2).

The highest catalytic activity, in terms of the specific current, is observed when a 15 mC/cm^2 of Ni has been electrodeposited onto the GC electrode as appeared in Fig. 5d. After modifying the Ni/GC electrode with CuOx, Ni-Cu/GC electrode, the specific current increased from 340 to 409 Ag^{-1} indicating the facilitated GO at the binary Ni-Cu catalyst (Fig. 6).

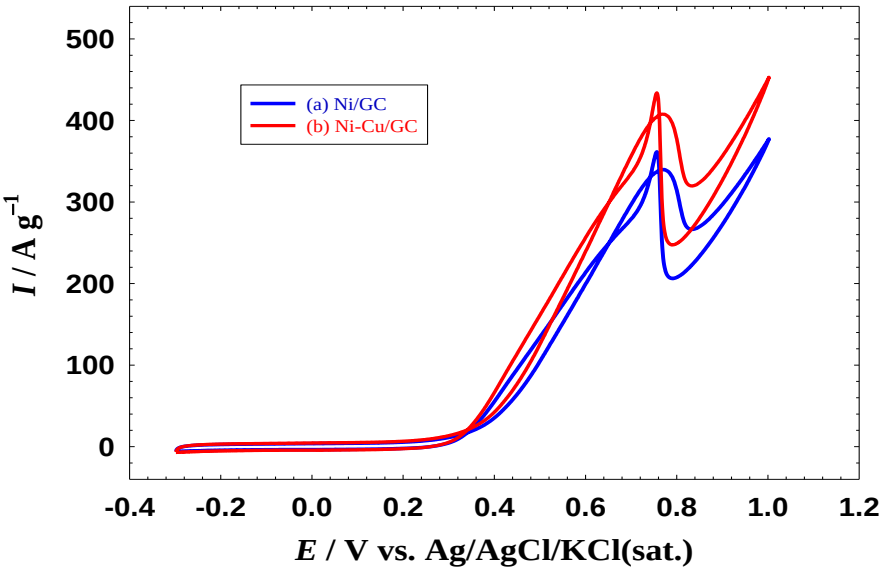

Figure 6. CVs measured in 0.5 M NaOH solution containing 50 mM glucose at a scan rate of 100 mVs^{-1} for (a) Ni/GC and (b) Ni-Cu/GC electrodes at which a mC/cm^2 of Ni has been electrodeposited.

Another objective from adding the CuOx to the Ni/GC electrode is to improve the stability towards GO. So, the anodic oxidation current of glucose has been recorded at a constant potential of 0.6 V for a prolonged electrolysis time of ca. 1 h for the Ni/GC (Fig. 7a) and Ni-Cu/GC (Fig. 7b) electrodes. Again, matching with the data in Fig. 6, the Ni-Cu/GC electrode shows a higher stability in terms of maintaining a high specific current value during the continuous electrolysis.

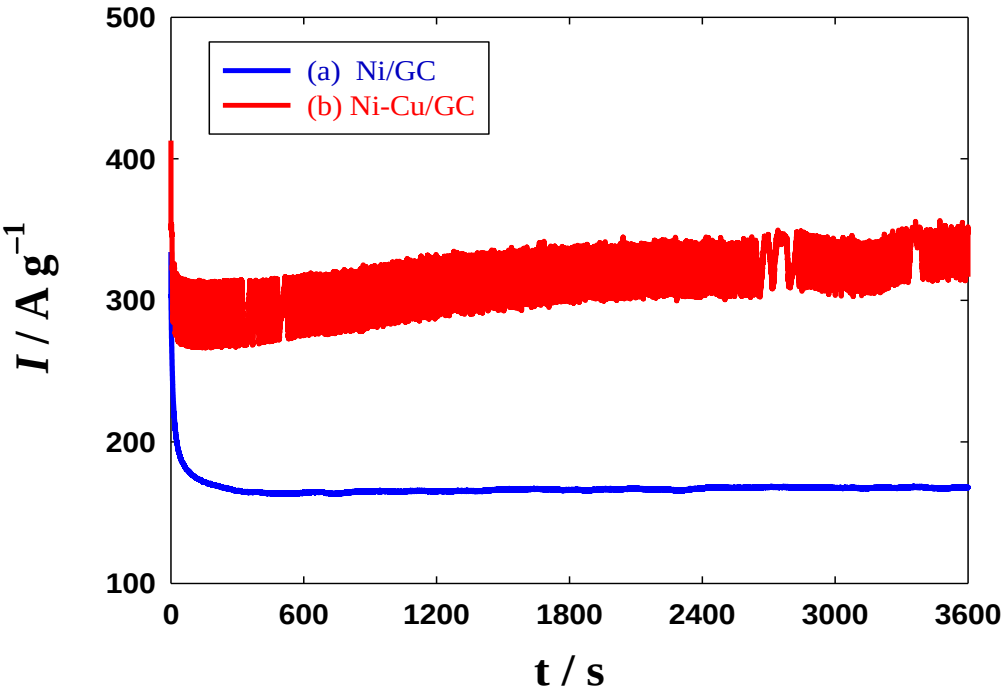

Figure 7. Current-time relation measured in 0.5 M NaOH solution containing 50 mM glucose at a constant potential of 0.6 V for (a) Ni/GC and (b) Ni-Cu/GC electrodes at which a 15 mC/cm^2 of Ni has been electrodeposited.

4. CONCLUSION

A binary catalyst composed of NiOx and CuOx has been fabricated over a GC surface and characterized using FE-SEM, EDS and XRD. The optimization of the Ni deposition charge has been performed and a 15 mC/cm^2 was sufficient to acquire the highest catalytic activity in terms of the specific current (340 Ag^{-1}). Then the Ni/GC electrode has been modified with CuOx that further improved the catalytic activity (409 Ag^{-1}) and the stability (two folds higher specific current after 1 h of continuous electrolysis) towards GO.

References

1. I. M. Al-Akraa, A. M. Mohammad, M. S. El-Deab, B. E. El-Anadouli, *Arab. J. Chem.*, 10 (2017) 877.
2. I. M. Al-Akraa, T. Ohsaka, A. M. Mohammad, *Arab. J. Chem.*, 12 (2019) 897.

3. B. A. Al-Qodami, H. H. Farrag, S. Y. Sayed, N. K. Allam, B. E. El-Anadouli, A. M. Mohammad, *J. Nanotechnol.*, 2018 (2018)
4. M. S. El-Deab, G. A. El-Nagar, A. M. Mohammad, B. E. El-Anadouli, *J. Power Sources*, 286 (2015) 504.
5. G. A. El-Nagar, M. S. El-Deab, A. M. Mohammad, B. E. El-Anadouli, *Electrochim. Acta*, 180 (2015) 268.
6. I. M. Al-Akraa, A. M. Mohammad, *Arab. J. Chem.*, (2019)
7. I. M. Al-Akraa, A. M. Mohammad, M. S. El-Deab, B. E. El-Anadouli, *J. Nanotechnol.*, 2018 (2018)
8. I. M. Al-Akraa, *Int. J. Hydrogen Energy*, 42 (2017) 4660.
9. I. M. Al-Akraa, Y. M. Asal, A. M. Mohammad, *J. Nanomater.*, 2019 (2019) Article ID 2784708.
10. I. M. Al-Akraa, A. M. Mohammad, M. S. El-Deab, B. E. El-Anadouli, *Int. J. Electrochem. Sci.*, 7 (2012) 3939.
11. I. M. Al-Akraa, A. M. Mohammad, M. S. El-Deab, B. E. El-Anadouli, *J. Electrochem. Soc.*, 162 (2015) F1114.
12. I. M. Al-Akraa, A. M. Mohammad, M. S. El-Deab, B. E. El-Anadouli, *Int. J. Hydrogen Energy*, 40 (2015) 1789.
13. I. M. Al-Akraa, A. M. Mohammad, M. S. El-Deab, B. E. El-Anadouli, in *Progress in Clean Energy, Volume 1: Analysis and Modeling*. (2015), pp. 551-558.
14. I. M. Al-Akraa, A. M. Mohammad, M. S. El-Deab, B. S. El-Anadouli, *Int. J. Electrochem. Sci.*, 10 (2015) 3282.
15. Y. M. Asal, I. M. Al-Akraa, A. M. Mohammad, M. S. El-Deab, *Int. J. Hydrogen Energy*, 44 (2019) 3615.
16. Y. M. Asal, I. M. Al-Akraa, A. M. Mohammad, M. S. El-Deab, *J. Taiwan Inst. Chem. Eng.* 96 (2019) 169.
17. A. M. Mohammad, I. M. Al-Akraa, M. S. El-Deab, *Int. J. Hydrogen Energy*, 43 (2018) 139.
18. I. M. Al-Akraa, A. M. Mohammad, M. S. El-Deab, B. E. El-Anadouli, *Int. J. Electrochem. Sci.*, 8 (2013) 458.
19. A.Samphao, P. Butmee, J. Jitcharoen, L. Svorc, G. Raber, K. Kalcher, *Talanta*, 142 (2015) 35.
20. S. C. Barton, J. Gallaway, P. Atanassov, *Chem. Rev.*, 104 (2004) 4867.
21. S. C. Barton, H. H. Kim, G. Binyamin, A. Heller, *J. Am. Chem. Soc.*, 123 (2001) 5802.
22. R. A. Bullen, T. C. Arnot, J. B. Lakeman, F. C. Walsh, *Biosens. Bioelectron.*, 21 (2006) 2015.
23. M. Ghasemi, M. Ismail, S. K. Kamarudin, K. Saeedfar, W. R. W. Daud, S. H. A. Hassan, L. Y. Heng, J. Alam, S. E. Oh, *Appl. Energy*, 102 (2013) 105.
24. H. H. Kim, Y. C. Zhang, A. Heller, *Anal. Chem.*, 76 (2004) 2411.
25. P. Pandey, V. N. Shinde, R. L. Deopurkar, S. P. Kale, S. A. Patil, D. Pant, *Appl. Energy*, 168 (2016) 706.
26. S. Shleev, J. Tkac, A. Christenson, T. Ruzgas, A. I. Yaropolov, J. W. Whittaker, L. Gorton, *Biosens. Bioelectron.*, 20 (2005) 2517.
27. J. Chen, H. Zheng, J. Kang, F. Yang, Y. Cao, M. Xiang, *RSC Adv.*, 7 (2017) 3035.
28. K. Rabaey, N. Boon, S. D. Siciliano, M. Verhaege, W. Verstraete, *Appl. Environ. Microbiol.*, 70 (2004) 5373.
29. A. M. Mohammad, A. I. Abdelrahman, M. S. El-Deab, T. Okajima, T. Ohsaka, *Colloids Surf. A Physicochem. Eng. Asp.*, 318 (2008) 78.
30. A. M. Mohammad, S. Dey, K. K. Lew, J. M. Redwing, S. E. Mohney, *J. Electrochem. Soc.*, 150 (2003) G577.
31. A. M. Mohammad, T. A. Salah Eldin, M. A. Hassan, B. E. El-Anadouli, *Arab. J. Chem.*, 10 (2017) 683.

32. I. M. Sadiek, A. M. Mohammad, M. E. El-Shakre, M. S. El-Deab, B. E. El-Anadouli, *J. Solid State Electrochem.*, 17 (2013) 871.
33. M. S. El-Deab, L. A. Kibler, D. M. Kolb, *Electrochem. Commun.*, 11 (2009) 776.
34. I. M. Al-Akraa, Y. M. Asal, S. D. Khamis, *Int. J. Electrochem. Sci.*, 13 (2018) 9712.
35. G. A. El-Nagar, A. M. Mohammad, M. S. El-Deab, B. E. El-Anadouli, *Electrochim. Acta*, 94 (2013) 62.
36. M. Raffi, S. Mehrwan, T. M. Bhatti, J. I. Akhter, A. Hameed, W. Yawar, M. M. u. Hasan, *Ann. Microbiol.*, 60 (2010) 75.
37. A. M. Ahmed, S. Y. Sayed, G. A. El-Nagar, W. M. Morsi, M. S. El-Deab, B. E. El-Anadouli, *J. Electroanal. Chem.*, 835 (2019) 313.